

Integrated platform to design robust energy internet

Zhengchao Wang^a, A. T. D. Perera^b

^a*Imperial College Business School, Imperial College London, London, SW7 2AZ, UK*

^b*Solar Energy and Building Physics Laboratory, EPFL, CH-1015 Lausanne, Switzerland*

Abstract

This study proposes a novel method to address the design problem of the energy internet (EI). The novel approach consists of a Pareto multi-objective optimization of the distributed energy system (DES) and a bi-level DES configuration and grid design, which guarantees n-1 security through a robust stochastic optimization model. The model is tested using two case studies. The results reveal that the novel approach can yield the optimal combination of the DES configurations and the grid design for the EI, which reduces the overall cost up by to 60% when compared to methods with separate optimization of each system and the grid (as is common in the present state-of-the-art). The study reveals that EI design is sensitive to locations of the demand and their intensity and to the cost of the grid, which makes it difficult to use a simple algorithm such as the minimum/weighted spanning tree. Moreover, the novel method ensures n-1 security of the EI, which decreases the loss of load probability (LoLP) by up to 45%. The approach introduced in this study can be used to design future urban EIs with robust operation and improved interaction among the DESs.

Keywords: energy internet, distributed energy system, grid optimization, robust stochastic optimization, n-1 security

¹ **Nomenclature**

² **Acronym**

³ CSR Cost saving ratio

⁴ DES Distributed energy system

⁵ EI Energy Internet

⁶ LCC Life-cycle cost

⁷ LoLP Loss of load probability

⁸ **Objectives**

⁹ $H(\mathbf{D}_Z)$ Grid cost function given the demand profiles \mathbf{D}_Z

¹⁰ **Parameters**

¹¹ \bar{i} Total number of DESs within the EI

¹² \mathbf{D}_Z Demand profiles of energy systems under configuration Z

¹³ $c^g(Z)$ Life-cycle cost of the grid under system configuration Z

¹⁴ c_{ik}^s Life-cycle cost of energy system configuration k for neighbourhood i

¹⁵ cf_{ij} Fix cost of grid line ij

¹⁶ cl_{ij} Cost of single connection circuit between node i and node j

¹⁷ d_i^t Demand at node i at time t

¹⁸ f_{ij}^{cap} Capacity of single circuit between node i and node j

- ¹⁹ g_i^{max} Maximal power that can be generated from node i
- ²⁰ g_i^{min} Minimal power that can be generated from node i
- ²¹ k_i Total number of Pareto optimal configurations for DES i
- ²² m_{ij} Maximum number of circuits that can be installed between node i and
²³ node j
- ²⁴ p Penalty of unit curtailment of demand
- ²⁵ x_{ij}^{max} Maximum allowed number of circuits between node i and node j
- ²⁶ x_{ij}^{min} Minimal allowed number of circuits between node i and node j

²⁷ **Sets**

- ²⁸ Θ Set of all potential connections among DESs
- ²⁹ \mathbb{C} Set of grid connection contingency scenarios
- ³⁰ \mathbb{H} Set of the years considered
- ³¹ \mathbb{I} Set of DESs of interest
- ³² \mathbb{K}_i Set of configurations of DES i
- ³³ \mathbb{N} Set of non-negative integers
- ³⁴ \mathbb{T} Set of time steps considered
- ³⁵ \mathbf{S} Set of all components installed in DES

³⁶ **Variables**

³⁷	\mathbf{p}_{it}	Position of particle i at step t
³⁸	\mathbf{p}_{it}^{best}	Best position found by particle i till step t
³⁹	\mathbf{p}_t^{best}	Best position found by all particles till step t
⁴⁰	\mathbf{v}_{it}	Velocity of particle i at step t
⁴¹	\mathbf{x}	Grid connection of the whole system
⁴²	\mathbf{x}^c	Grid connection of the whole system under contingency c
⁴³	\mathbf{y}^{tc}	Power flow analysis variables at time t under contingency c
⁴⁴	\mathbf{Z}	Matrix integration of configuration indicator variable \mathbf{Z}_{ik}
⁴⁵	\mathbf{Z}_{ik}	Indicator variable if neighbourhood i chooses energy system configuration k
⁴⁶		
⁴⁷	f_{ij}^{tc}	Power flow from node i to node j at time t under contingency c
⁴⁸	g_i^{tc}	Power generated from node i at time t under contingency c
⁴⁹	l_{ij}	binary index if the grid line between node i and node j is chosen
⁵⁰	r_i^{tc}	Curtailment of demand or generation at node i at time t under contingency c
⁵¹		
⁵²	x_{ij}	Number of circuits between node i and node j
⁵³	x_{ij}^c	Number of circuits between node i and node j under contingency c

54 **1. Introduction**

55 Renewable energy integration plays an important role in the fight against
56 climate change (Le Guen et al., 2018). Owing to the intermittent nature of
57 solar photovoltaic (SPV) and wind energy, large-scale integration of these
58 energy technologies directly into the grid on large scale is challenging. Dis-
59 tributed energy systems (DESs) (Perera et al., 2017a,b) such as energy hubs
60 are an attractive solution to facilitate large-scale integration of non-dispatchable
61 renewable energy technologies. However, it is difficult to extend the design of
62 a single DES to that of the energy internet (EI), which can be regarded as a
63 network of DESs. EI design requires optimization of both DESs and the grid.
64 Both design and operation of DES within the EI are strongly influenced by
65 the grid interactions. Similarly, optimizing the connectivity (grid) within an
66 EI requires the interaction of DESs within that EI. Thus, EI design is difficult
67 because of the mutual coupling between the DES configuration and the grid.
68 In the current two-step independent EI design process, which first designs
69 the DESs and then the grid, the optimal combination cannot be determined
70 due to this mutual dependence. Moreover, it is essential to guarantee the
71 robust operation of the EI considering stochastic demands, generations, and
72 failure in the grid ($n-1$ security), which increases the difficulty of the design
73 process. To address these challenges, we evaluate the present state-of-the-art
74 in the next section in order to determine a promising way forward.

75 *1.1. Distributed energy system optimization*

76 A number of recent studies have focused on the optimal design of stand-
77 alone and grid-integrated DESs (Jing et al., 2019, Lorestani and Ardehali,

78 2018a,b). The cost of a stand-alone energy system is significantly high when
79 compared to the grid-integrated systems (Gharavi et al., 2015). Although
80 several recent studies focused on the design optimization of grid-integrated
81 DESs, these studies simply overlooked the grid curtailments. For example,
82 Varasteh et al. (2019), Ren et al. (2018), Majewski et al. (2017), Li et al.
83 (2016) optimized the DES assuming the grid to be an infinite source or sink.
84 This may result in a system design that has large-scale injection or extraction
85 of electricity, leading to cascade failures in the grid. Therefore, the constraint
86 for grid interaction plays a vital role when designing DESs, as shown by
87 Jreddi et al. (2019) and Morvaj et al. (2016). More importantly, Morvaj et
88 al. observed that considering grid curtailments can have a notable impact on
89 the sizing of energy systems. Perera et al. (2017a) proposed a multi-objective
90 DES design model using the life-cycle cost (LCC) and the DES autonomy
91 level as objectives. Their proposed approach can be used to obtain a Pareto
92 frontier of the cost and the autonomy level of DES design. However, it is
93 difficult to derive the optimal grid connectivity from the perspective of a
94 single energy system. This is because the optimal design depends on the
95 power requirement of energy systems that are connected to the grid. Hence,
96 it is important to see the problem from a wider perspective.

97 *1.2. Grid optimization*

98 From the grid optimization perspective, a number of models have been
99 proposed to guarantee reliable operation of the grid, which is considered a ma-
100 jor challenge (especially with renewable energy integration). The approaches
101 employed for designing the grid under uncertainties can be categorized into
102 robust optimization (Vilaça Gomes et al., 2019, Mishra et al., 2019, Jabr,

103 stochastic optimization (Lumbreras et al., 2017), and chance con-
104 straint optimization (Yu et al., 2009, Yang and Wen, 2005). During the
105 design process, robust optimization only considers the worst scenario. Wu
106 et al. (2008) showed that the worst scenario for the grid takes place at the
107 lower or the upper bound of uncertain demands and generations, which no-
108 tably simplifies the model (Mínguez and García-bertrand, 2016, Roldán et al.,
109 2018). However, the grid designed by robust optimization can be very con-
110 servative (resources are not utilized most of the time), because the worst
111 scenarios rarely happen. To overcome this shortcoming, stochastic optimiza-
112 tion methods strike a balance among a series of scenarios that have different
113 levels of occurrence probability. The chance constraint methods allow a spe-
114 cific probability that the grid capacity constraint is violated. However, both
115 stochastic and chance constraint optimization are analytically intractable in
116 most instances (Zymler et al., 2013). As a result, simulation-based approx-
117 imation techniques are introduced to address this intractability in practice
118 (Lumbreras et al., 2017, Yu et al., 2009, Yang and Wen, 2005). However, the
119 approximation precision of simulation-based techniques is limited because of
120 the “curse of dimensionality” (Bengtsson et al., 2008, Wang and Fang, 2003).

121 Imposing n-K security, which is a property that allows the system to op-
122 erate reliably under a loss of k components, is a common way to design a
123 reliable grid (Lumbreras et al., 2017, Moreira et al., 2017, Orfanos et al.,
124 2013). However, enforcing n-K security increases the complexity of the grid
125 design problem, because a set of operation constraints must be added for each
126 potential contingency. In summary, on one hand, the approaches used to de-
127 sign DESs oversimplify the interactions with the grid in the design phase.

128 On the other hand, grid optimization techniques are already exhaustive, es-
129 pecially when considering uncertainties. Therefore, it is difficult to extend
130 these methods directly to optimize a robust EI where both DESs and the
131 grid are to be considered.

132 *1.3. Contribution*

133 Although EIs are of great interest due to their potential to integrate
134 distributed renewable energy technologies, it is challenging to design EIs
135 while guaranteeing robust operation. This study attempts to address this
136 research problem by introducing the following:

- 137 1. An integrated EI optimization model. The optimization model can
138 be used to simultaneously design DESs and the grid connecting these
139 systems.
- 140 2. A n-1 secured robust stochastic grid optimization model is introduced
141 to guarantee reliable operation of the system while being less conser-
142 vative. An hourly time series simulation and power flow are conducted
143 when optimizing the DES and the grid, respectively. This guarantees
144 smooth operation of systems by taking into account the short term and
145 seasonal fluctuations in the demand and renewable energy potentials.
- 146 3. A comprehensive assessment is conducted to evaluate the impacts of
147 the inter-coupling between the grid and DESs and its influences on the
148 design (considering the sensitivity to grid cost and to the locations of
149 DESs) and the security of the EI.

150 The manuscript is organized as follows. Section 2 describes the proposed
151 mathematical model, while Section 3 introduces the optimization framework.

₁₅₂ Finally, the obtained results are presented in Section 4 and Section 5 presents
₁₅₃ the conclusions of this study.

₁₅₄ **2. Mathematical modeling**

₁₅₅ For a future EI with large-scale integration and sharing of renewable en-
₁₅₆ ergy sources among DESs, an integrated design of multiple DESs and the
₁₅₇ grid is important in order to avoid a sub-optimal solution and extra cost
₁₅₈ (Roldán et al., 2018). However, optimizing such an EI is difficult because of
₁₅₉ the aforementioned interaction among DESs and the grid. To model these
₁₆₀ complex interactions with reasonable accuracy, we assume that DESs within
₁₆₁ the considered EI are cooperative in the design phase. Through this assump-
₁₆₂ tion, EI design can be divided into two steps. In the first step, a Pareto
₁₆₃ multi-objective optimization of the DES is conducted considering cost and
₁₆₄ the intensity of grid integration levels as objective functions. The second step
₁₆₅ consists of bi-level DES configuration selection (from configurations obtained
₁₆₆ using the Pareto optimization in the first step) and the grid design problem,
₁₆₇ each of which is significantly smaller and easier, as shown in Fig. 1.

₁₆₈ The proposed model begins with Pareto multi-objective optimization of
₁₆₉ the DES within the EI (Step 1). The configurations of DES i are obtained
₁₇₀ by considering its energy demand of the building stock, wind, and solar PV
₁₇₁ energy potential on an hourly scale, which is explained briefly in Section 2.1.
₁₇₂ The resulting configurations that are on the Pareto front are recorded into
₁₇₃ configuration set K_i and labeled numerically with a descending life-cycle cost
₁₇₄ (LCC). In the next step (Step 2), a bi-level problem is formulated to opti-
₁₇₅ mize the EI. The first level, described in detail in Section 2.2.1, selects one

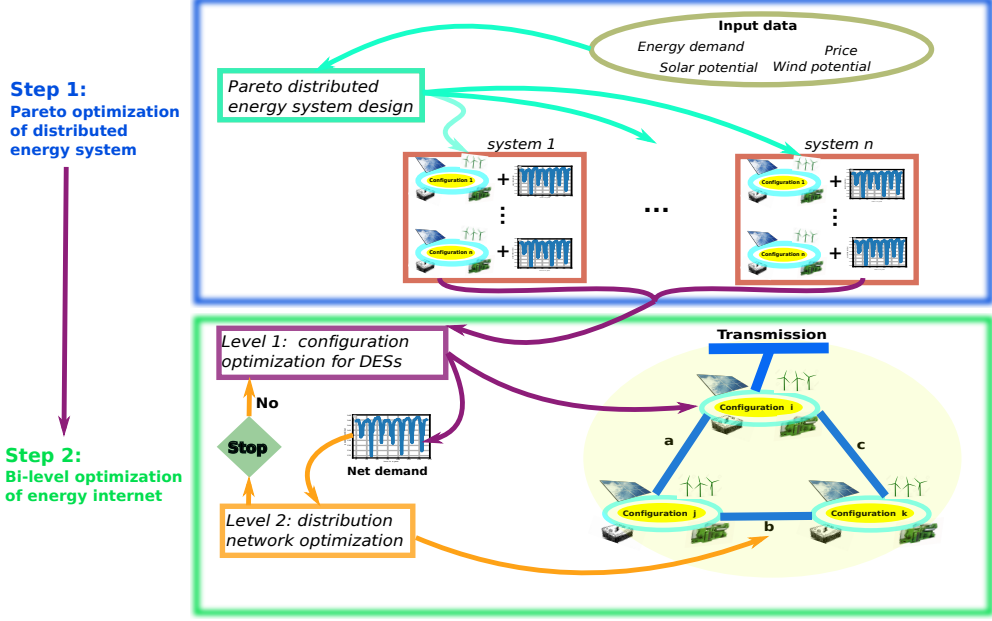


Figure 1: Illustration of the proposed two-step integrated Energy Internet optimisation model

176 configuration per DES and computes the total LCC of the DESs. The second
 177 level, described in Section 2.2.2, takes the net demand profiles of chosen con-
 178 figurations as inputs and optimizes the LCC while guaranteeing $n-1$ security
 179 for the grid. In the end, the DES configurations and the corresponding grid,
 180 whose overall LCC is the smallest, are reported as the optimal EI.

181 *2.1. Pareto multi-objective optimisation of the DES*

182 The Pareto multi-objective optimization model proposed by Perera et al.
 183 (2017a) is conducted to optimize the configurations of each DES (Step 1)
 184 considering two conflicting objectives, namely the LCC of the system and
 185 the grid curtailment. The model takes hourly solar irradiation, wind speed,
 186 energy demand data, and techno-economic details of the system components

187 as inputs. The model outputs parameters (the capacity of wind turbines,
188 solar PV panels, internal combustion generator, and battery bank) and the
189 operation strategy (operating load factor of the internal combustion genera-
190 tor, and the energy interactions between battery bank and the grid) of the
191 minimal-cost energy system under different grid interaction strengths. In
192 other words, the model output DES configurations lie on the Pareto frontier
193 of LCC and grid interaction strength.

194 The decision space variables are mapped into the objective space through
195 a time series simulation of the energy system. At each time step, a bi-level
196 dispatch strategy is used to manage the energy flow within the system. The
197 primary level of the dispatch strategy determines the operating load factor
198 of the generator based on fuzzy logic. Subsequently, finite state automata
199 theory is used to determine the interactions between the battery bank and
200 the grid. Through the simulation, the energy system operation and mainte-
201 nance cost can be determined, which consists of a fixed cost (OM_s^F) and a
202 replacement cost (RC_s) of components. Similarly, the cost for grid interac-
203 tions (CGI) can be obtained, which is the net cost of electricity purchased
204 from and injected into the grid considering the real time cost of energy in
205 the transmission grid. The initial capital cost (ICC) of the system consists
206 of acquisition cost for system components and the installation cost. For a
207 detailed description of the model, please refer to the article by Perera et al.
208 (2017a). Finally, the present value of all the cash flows are considered as the
209 life-cycle cost of energy system (LCC_s), whose computation formula is given
210 by Eq. (1).

$$LCC_s = ICC + \sum_{s \in \mathbb{S}} OM_s^F CRF_s + \sum_{h \in \mathbb{H}} \sum_{s \in \mathbb{S}} p_s^h RC_s + CGI \quad (1)$$

211 In this equation, CRF_s denotes Capital Recovery Factor for component s for
 212 operation and maintenance. p_s^h denotes the real interest rate calculated using
 213 both interest rates for investment and local market annual inflation ratio. \mathbb{H}
 214 denotes the set of life span.

215 Minimizing the interactions maintained with the grid to improve the au-
 216 tonomy of the DES is often discussed in the present state-of-the-art (Perera
 217 et al., 2017a, 2018, Le Guen et al., 2018). According to the literature, auton-
 218 omy can be defined in several different ways. In this study, curtailments set
 219 (CS) for selling and purchasing electricity to and from the grid are related to
 220 the autonomy of the system. The capacity for injecting excess energy (CI_t)
 221 and purchasing electricity from the grid (CP_t) at time t is considered as an
 222 objective function, which is minimised along with the LCC_s according to Eq.
 223 (2).

$$CS = \max (\max (CI_t), \max (CP_t)) \quad (2)$$

224 The time series simulation through a Markov decision process formulates
 225 neither linear nor convex functions. Hence, it is required to move into a
 226 heuristic method to conduct Pareto optimization. Steady state epsilon dom-
 227 inance technique (Li et al., 2011), which has shown better performance during
 228 optimization for engineering problems, is used in this study to conduct the
 229 DES optimization.

230 2.2. Bi-level DESs configuration and grid design

231 Based on the Pareto optimal configurations of all DESs within the EI,
232 this section presents a novel LCC minimized bi-level DES configuration and
233 grid design model. The first level of the model determines the configuration
234 combination of all DESs, while the second level optimizes a robust grid for
235 the EI.

236 2.2.1. Optimization of distributed energy system configuration

237 Suppose that there are I DESs (denoted by set $\mathbb{I} = \{1, 2, \dots, I\}$), the
238 Pareto optimal configuration set of DES i optimised by the model presented
239 in Section 2.1 is denoted as $\mathbb{K}_i = \{1, \dots, k_i\}$. For configuration k of DES i ,
240 the notations of its LCC and net demand profile through the considered time
241 horizon \mathbb{T} are c_{ik}^s and \mathbf{d}_{ik} , respectively. Note that, unlike the considered tra-
242 ditional demand profile, \mathbf{d}_{ik} could also have negative elements, representing
243 the energy injection into the grid by DES i .

244 The optimal configuration combination of DESs is formulated as shown
245 by Eqs. (3) to (6). The decision variables are encapsulated into \mathbf{Z} , a ma-
246 trix of DES configuration indicators with each row representing one DES.
247 Equation (3) is the objective function, which is split into two parts: LCC re-
248 lated to DESs and that related to construction of the supporting grid $c^g(\mathbf{Z})$.
249 Constraint (4) specifies that the configuration indicator variable is binary,
250 equaling to one if it is chosen and zero otherwise. Constraint (5) specifies
251 that exactly one configuration should be chosen for one DES. For each con-
252 figuration choice \mathbf{Z} , the corresponding net demand profiles $\mathbf{D}_\mathbf{Z}$ is obtained,
253 according to which function $H(\mathbf{D}_\mathbf{Z})$ gives the grid cost (6) depending on the
254 demand profiles. The determination of this cost function is given in the next

255 section.

$$\min_{\mathbf{Z}} \quad \sum_i \sum_k c_{ik}^s \mathbf{Z}_{ik} + c^g(\mathbf{Z}) \quad (3)$$

$$\text{s.t. } \mathbf{Z}_{ik} \in \{0, 1\} \quad \forall i \in \mathbb{I} \quad \forall k \in \mathbb{K}_i \quad (4)$$

$$\sum_k \mathbf{Z}_{ik} = 1 \quad \forall i \in \mathbb{I} \quad (5)$$

$$c^g(\mathbf{Z}) \geq H(\mathbf{D}_{\mathbf{Z}}) \quad (6)$$

256

257 *2.2.2. Grid connection model for DESs*

258 This section presents a grid design model and the determination of the
259 LCC of the grid $H(\mathbf{D}_{\mathbf{Z}})$. The model aims at designing a grid that is robust to
260 random connection contingency (n-1 reliability) and stochastic generations
261 and demands. In this model, each DES is regarded as a node (bus). The
262 corresponding grid optimization model is then given by Eqs (7) to (15).

263 This model is built upon the flow-based optimal power flow model, as
264 discussed by Romero et al. (2002) for the computational simplicity (López
265 et al., 2012, Álvarez López et al., 2013, Alvarez et al., 2018, Gong et al.,
266 2018). The objective function (7) minimizes the sum of LCC of the grid and
267 the largest penalty for lost load or generation curtailment among all time
268 periods \mathbb{T} under all contingency scenarios \mathbb{C} . Constraint (8) specifies that
269 the connectivity of line ij connecting node i and node j is a binary variable
270 ($l_{ij} = 1$ if connected, 0 otherwise). Constraint (9) and (10) regulate the
271 feasible region of the grid capacity variables x_{ij} . It is a non-negative integer
272 upper bounded by the connectivity multiplied by constant m_{ij} which can

273 be chosen as desired to limit the number of circuits that can be installed in
 274 practice. Constraints (11) to (15) are used for the power flow analysis at
 275 time t under the contingency scenario c to compute the total loss of load
 276 or generation curtailment $\sum_i |r_i^{tc}|$. For the simplification of notation, we
 277 use d_i^t to represent the power demand of node i at time t under the DESs
 278 configurations choice \mathbf{Z}

$$\min_{l_{ij}, x_{ij}} \quad \left(\sum c f_{ij} l_{ij} + \sum c l_{ij} x_{ij} + \max_{t,c} \min_{\mathbf{f}^{tc}, \mathbf{g}^{tc}, \mathbf{r}^{tc}} p \sum_{i=1}^n |r_i^{tc}| \right) \quad (7)$$

$$\text{s.t. } l_{ij} \in \{0, 1\} \quad \forall ij \in \Theta \quad (8)$$

$$x_{ij} \in \mathbb{N} \quad \forall ij \in \Theta \quad (9)$$

$$0 \leq x_{ij} \leq m_{ij} l_{ij} \quad \forall ij \in \Theta \quad (10)$$

$$|f_{ij}^{tc}| \leq x_{ij}^c f_{ij}^{cap} \quad \forall ij \in \Theta, \forall t \in \mathbb{T}, \forall c \in \mathbb{C} \quad (11)$$

$$\sum_{j \in \mathbb{N}(i)} f_{ij}^{tc} + g_i^{tc} + r_i^{tc} = d_i^t \quad \forall i \in \mathbb{I}, \forall t \in \mathbb{T}, \forall c \in \mathbb{C} \quad (12)$$

$$g_i^{tc} \in [g_i^{min}, g_i^{max}] \quad \forall i \in \mathbb{I}, \forall t \in \mathbb{T}, \forall c \in \mathbb{C} \quad (13)$$

$$0 \leq r_i^{tc} \leq d_i^t \quad \text{if } d_i^t \geq 0 \quad \forall i \in \mathbb{I}, \forall t \in \mathbb{T} \quad (14)$$

$$0 \geq r_i^{tc} \geq d_i^t \quad \text{if } d_i^t < 0 \quad \forall i \in \mathbb{I}, \forall t \in \mathbb{T} \quad (15)$$

279
 280 For a DES with generation infrastructures, the interval of curtailed vari-
 281 able r_i^{tc} must be specified according to the sign of d_i^t . In this model, d_i^t is
 282 non-negative if DES i takes energy from the grid at time t , and negative
 283 in case energy is injected into the grid. Therefore, the normal constraint
 284 $0 \leq r_i^{tc} \leq d_i^t$ is no longer valid when d_i^t is negative. Thus, the normal con-
 285 straint is split into constraints (14) and (15). Because of the same reason,

286 an absolute value operator is applied to r_i^{tc} in the objective function (7) to
287 penalise generation curtailment. These constraints and objective function
288 seem to lead to a non-linear problem. However, because d_i^t is exogenous to
289 the problem, a linear program can be derived for each realization of d_i^t .

290 Distinct from the existing robust grid optimization, where the bounds of
291 demand at different nodes are assumed (Jabr, 2013), this study directly uses
292 hourly demand profiles to guarantee the robustness of the designed grid. In
293 particular, assuming that demand profiles have T_m measured data points,
294 $\mathbf{d}^t = [d_1^t, \dots, d_I^t]^T$, $t \in \mathbb{T} = \{1, \dots, T_m\}$, the robustness of the grid to stochas-
295 tic net demands is guaranteed if $\sum_i p|r_i^{tc}| = 0 \forall t \in \mathbb{T}$, i.e. $\max_{t \in \mathbb{T}} \sum_i p|r_i^{tc}| = 0$.
296 On top of this, the robustness of the grid under contingency is also ensured
297 if $\max_{c \in \mathcal{C}} \max_{t \in \mathbb{T}} \sum_i p|r_i^{tc}| = 0$. As claimed by Yu et al. (2009), when the penalty
298 factor p is assigned properly, $\max_{c \in \mathcal{C}} \max_{t \in \mathbb{T}} \sum_i p|r_i^{tc}| = 0$ will be zero when the
299 optimization is complete. We term this novel model as the n-1 secured robust
300 stochastic grid optimization model.

301 Compared with existing models that we have reviewed, the novel grid
302 optimization model has the following advantages. In contrast to robust op-
303 timization, the proposed model is less-conservative as it is only robust to
304 realized demands and generations rather than the worst combination of un-
305 certain ones. This implies that correlations among demands and generations
306 are incorporated implicitly. Compared with stochastic optimization, the dif-
307 ference lies in the objective function. While the expectation or quantile of
308 curtailment penalty is usually adopted in stochastic program-based grid de-
309 sign models, the worst curtailment penalty is adopted in our model. Because
310 of this worst operator, techniques can be applied to narrow down numerous

311 scenarios to some dominant cases. Then, only operation constraints need to
 312 be performed on these dominant cases, thus significantly reducing computa-
 313 tion time compared to stochastic programs. In summary, the model achieves
 314 (with tractable complexity) the design of a less conservative grid that is re-
 315 liable despite the joint occurrence of stochastic demands, generations, and
 316 random contingency.

317 *2.3. Integrated EI optimisation model*

318 We integrate the model in Step 2, presented in Sections 2.2.1 and 2.2.2
 319 and reformulate it into Eqs. (16) to (22). The objective function described
 320 in (16) minimises the overall LCC of EI. Constraints (17) and (18) are the
 321 same as (4) and (5). Constraint (19) corresponds to constraints (8) and (10);
 322 constraint (20) represents constraints (12) to (15); constraint (21) represents
 323 the constraint (11); constraint (22) includes constraint (9) and integer in-
 324 formation of constraint (8). In this formulation, \mathbf{x} denotes the connectivity
 325 and capacity of the grid network. variable \mathbf{y}^{tc} is the union of the variables
 326 in power flow analysis, i.e. $\mathbf{y}^{tc} = [\mathbf{f}^{tc}, \mathbf{g}^{tc}, \mathbf{r}^{tc}]$.

$$\min_{\mathbf{Z}, \mathbf{x}} \quad \sum_i \sum_k c_{ik}^s \mathbf{Z}_{ik} + \left(\mathbf{c}^T \mathbf{x} + \max_{t,c} \min_{\mathbf{y}^{tc}} \mathbf{p}^T |\mathbf{y}^{tc}| \right) \quad (16)$$

$$\text{s.t. } \mathbf{Z}_{ik} \in \{0, 1\} \quad \forall i \in \mathbb{K} \quad \forall k \in \mathbb{K} \quad (17)$$

$$\sum_k \mathbf{Z}_{ik} = 1 \quad \forall i \in \mathbb{K} \quad (18)$$

$$\mathbf{A}\mathbf{x} \leq \mathbf{a} \quad (19)$$

$$\mathbf{G}\mathbf{y}^{tc} \leq \mathbf{b}^t(\mathbf{Z}) \quad \forall t \in \mathbb{T}, \forall c \in \mathbb{C} \quad (20)$$

$$\mathbf{T}_c \mathbf{x} + \mathbf{Q}\mathbf{y}^{tc} \leq \mathbf{e} \quad \forall t \in \mathbb{T}, \forall c \in \mathbb{C} \quad (21)$$

$$\mathbf{x} \in \mathbb{N} \quad (22)$$

327

328 This problem is a bi-level problem with a two-stage stochastic program
 329 embedded. The upper level problem optimizes DES configuration \mathbf{Z} and gives
 330 the net demand profiles $\mathbf{D}_\mathbf{Z}$, which is embedded in $\mathbf{b}^t(\mathbf{Z})$, to the lower level
 331 grid optimisation problem. Parameters $\mathbf{A}, \mathbf{G}, \mathbf{T}_c, \mathbf{Q}, \mathbf{a}$ and \mathbf{e} can be derived
 332 from their corresponding constraints mentioned previously. Along with the
 333 Pareto multi-objective optimization of the DES, it forms the integrated EI
 334 optimization model.

335 **3. Optimization methods**

336 Following the introduction of the proposed mathematical model, this sec-
 337 tion discusses the solving algorithms for the model presented in Eqs. (16)
 338 to (22). As explained in Section 2.2.1, the DES configuration optimiza-
 339 tion model determines the net demand profiles, which are inputs to the grid op-
 340 timization problem. The net demand profile is the outcome of complex op-
 341 eration strategy of the chosen DES configuration \mathbf{Z} ; hence, it is difficult for
 342 the DES configuration optimization problem to obtain an analytic expression
 343 of the grid LCC on \mathbf{Z} . Therefore, a heuristic algorithm is more suitable for
 344 the DES configuration optimization problem. The particle swarm algorithm
 345 (PSA) (Kaveh, 2016) is adopted owing to its successful application to rele-
 346 vant problems (Poullikkas, 2015, Martel et al., 2016). For the second-level
 347 grid optimization problem, we applied Benders Decomposition (BD) owing to
 348 the structure of the problem, because BD has been widely applied to similar
 349 grid optimization problems (Binato et al., 2001).

3.1. Particle Swarm algorithm for multi energy system configuration optimization problem

In this problem, the position \mathbf{p}_{it} of particle i at step t represents the current DES configurations, and the velocity \mathbf{v}_{it} of particle i at step t represents the change in speed of the DESs. The initial particle position and velocity are chosen randomly and then updated iteratively according to Eqs. (23) and Formula (24) as suggested by Kaveh (2016). Parameter \bar{r}_1 and \bar{r}_2 are random numbers uniformly distributed in the interval $(0, 1)$ while c_1 and c_2 are two parameters representing the particle's confidence in itself and in the swarm.

$$\mathbf{p}_{it+1} = \mathbf{p}_{it} + \mathbf{v}_{it} \quad (23)$$

$$\mathbf{v}_{it+1} = \mathbf{v}_{it} + c_1 \bar{r}_1 (\mathbf{p}_t^{best} - \mathbf{p}_{i,t}) + c_2 \bar{r}_2 (\mathbf{p}_{i,t}^{best} - \mathbf{p}_{it}) \quad (24)$$

361 Note that \mathbf{p}_{it} and \mathbf{v}_{it} computed by Eq. (23) and Eq. (24) are real numbers
 362 while our solutions are represented by integers. To address this mismatch,
 363 the value is rounded to the closest integer (Twaha and Ramli, 2018, Lorestani
 364 and Ardehali, 2018a, Paliwal et al., 2014). This strategy is also adopted in
 365 this article.

367 3.2. Benders Decomposition

The core idea of BD is to decompose a large optimization problem into smaller ones so that they are easy to solve and parallelize. One prominent property of a BD-applicable problem is that it contains variables and constraints that are structurized and separable, as in the case of our proposed n-1 secured robust stochastic grid optimization model. The grid optimization

373 model is a two-stage problem. The first stage optimizes the grid network \mathbf{x}
 374 while the second stage performs optimal power flow analysis to determine
 375 the feasibility and optimality of \mathbf{x} . Given \mathbf{x} , the optimal power flow analysis
 376 problems are independent of the combination of demand realization \mathbf{d}^t and
 377 contingency scenario c , and they are therefore parallelizable. By applying
 378 the BD framework, the grid network optimization problem is decomposed
 379 into Stage 1 and Stage 2 problems.

Stage 1

$$\min_{\mathbf{x}} \quad \mathbf{c}^T \mathbf{x} + \gamma$$

$$\text{s.t.} \quad \mathbf{A}\mathbf{x} \leq \mathbf{a}$$

$$\gamma \geq f(\mathbf{x})$$

$$\mathbf{x} \in \mathbb{Z}_{\geq 0}$$

Stage 2

$$\forall t \in \mathbb{T}, \forall c \in \mathbb{C}$$

$$\min_{\mathbf{y}^{tc}} \quad \mathbf{p}^T \mathbf{y}^{tc}$$

$$\text{s.t.} \quad \mathbf{T}_c \mathbf{x} + \mathbf{Q} \mathbf{y}^{tc} \leq \mathbf{k}^c$$

$$\mathbf{G} \mathbf{y}^{tc} \leq \mathbf{h}^{tc}$$

380 In each iteration, Stage 1 optimizes the grid connections \mathbf{x} and penalty γ^* .
 381 Subsequently, these are passed into Stage 2 to check the optimality of \mathbf{x} .
 382 Because a curtailment is added to the optimal power flow model, the problem
 383 is always feasible, which eliminate the need for adding a feasible cut. As
 384 long as there is a combination of net demand and contingency such that
 385 the objective $\mathbf{P}^T \mathbf{y}^{tc}$ is greater than γ^* , the obtained grid connection \mathbf{x} is not

386 optimal, and an optimal cut is added to the first stage of the problem. For the
 387 convenience of adding the optimal cut, we transfer the Stage 2 problem into
 388 its dual problem, whose objective function is given by (25) and constraints
 389 are given by (26) to (27).

$$\max_{\lambda^{tc}, \phi^{tc}} (\mathbf{T}_c \mathbf{x} - \mathbf{k}^c)^T \lambda^{tc} - \mathbf{h}^{tcT} \phi^{tc} \quad (25)$$

$$\text{s.t. } -\mathbf{Q}^T \lambda^{tc} - \mathbf{G}^T \phi^{tc} = \mathbf{p} \quad (26)$$

$$\lambda^{tc} \geq \mathbf{0}, \quad \phi^{tc} \geq \mathbf{0} \quad (27)$$

390 For each combination of demand and contingency scenario, the dual prob-
 391 lem is solved accordingly. If the objective value is larger than the first stage
 392 optimal variable γ^* , an optimal cut, given by Eq. (28), is added to the first
 393 stage problem. λ_*^{tc} and ϕ_*^{tc} are the optimal solution of the dual problem.

$$\gamma \geq (\mathbf{T}_c \mathbf{x} - \mathbf{k}^c)^T \lambda_*^{tc} - \mathbf{h}^{tcT} \phi_*^{tc} \quad (28)$$

394 4. Results and Discussion

395 The novel approach introduced in this study is assessed through several
 396 case studies. The results obtained from these case studies are discussed in de-
 397 tail in this section, and the performance of the novel optimization algorithm
 398 is compared with those of other methods used in the present state-of-the-art.
 399 Two main case studies are conducted, with each having an EI consisting of
 400 five and nine DESs, as shown in Fig. 2. The case studies are conducted
 401 considering the climate conditions in Lund, a major city in Sweden. A de-
 402 tailed description about the case study is presented in Perera et al. (2019).

403 Subsequently, a comprehensive analysis is conducted in order to evaluate the
 404 sensitivity of the optimal planning on the grid cost (4.2.1) and energy system
 405 locations (4.2.2) and to investigate the impact of operation reliability on the
 406 design (4.3). The results obtained from the novel approach are compared
 407 with those of existing techniques to understand the contribution of the novel
 408 method.

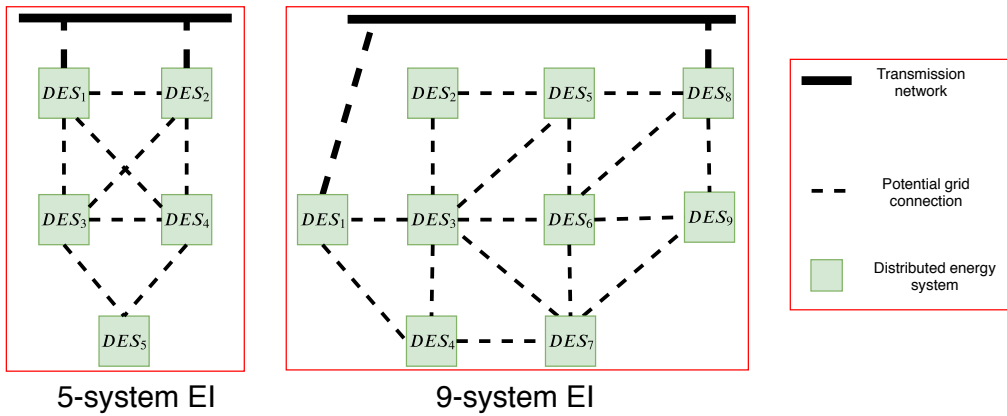


Figure 2: Topology and potential connections of the EI with five systems and nine systems. The distance between the transmission system and a grid-connected DES is 4 km, that between two horizontally or vertically connected DESs is 6 km, and that between diagonally connected DESs is 8.4 km

409 *4.1. Pareto optimal configurations of distributed energy system*

410 The first step in the optimization process is to derive the Pareto optimal
 411 design solutions for the DESs. Figure 3 presents the optimal solutions ob-
 412 tained for the nine DESs. Each point on the Pareto frontier represents one
 413 configuration, whose LCC and grid interaction strength are distinguished.
 414 When analyzing the Pareto fronts, a significant change in the LCC can be

415 observed among the systems. For example, the LCC of system 6 varies from
416 1.5 to 4.5 million dollars and that of system 3 ranges from 3 to 8.5 million
417 dollars. The changes in the LCC are not solely due to the changes in the scale
418 of the demand profile, but also due to changes in the shape of the demand
419 profile (caused by changes in the occupancy timing, level of refurbishment
420 in buildings, etc.) and the renewable energy potential. This indicates that
421 the leveled generation cost is not the same in all the locations. As a result,
422 it is profitable to be connected to neighboring energy systems that generate
423 electricity at a cheaper cost. However, the level of interaction among DESs
424 depends on the cost of connectivity and changes in the generation cost of the
425 neighbor (linked with the design of the energy system). Therefore, it is im-
426 portant to optimize both the network and the design of DESs simultaneously,
427 which is considered as the EI optimization problem in this study.

428 Moreover, the LCC decreases with the increase in the grid interaction
429 strength (CS) for a given system. The increased CS demands for a larger
430 grid capacity, which increases the cost of the grid construction. As indicated
431 by the Pareto frontier, the saved cost of the DES becomes marginal as the
432 grid interaction strength increases. This implies that there should be a point
433 where the increase in the grid cost is the same as the decrease in the sys-
434 tem LCC, i.e., where the minimal overall LCC is achieved. This evidence
435 motivates the economic benefit of integrated EI optimization. Without loss
436 of generality, this article chooses 25 configurations for each DES (labeled
437 from 1 to 25) with a decreasing life-cycle cost, as inputs to the bi-level DESs
438 configuration and grid design model.

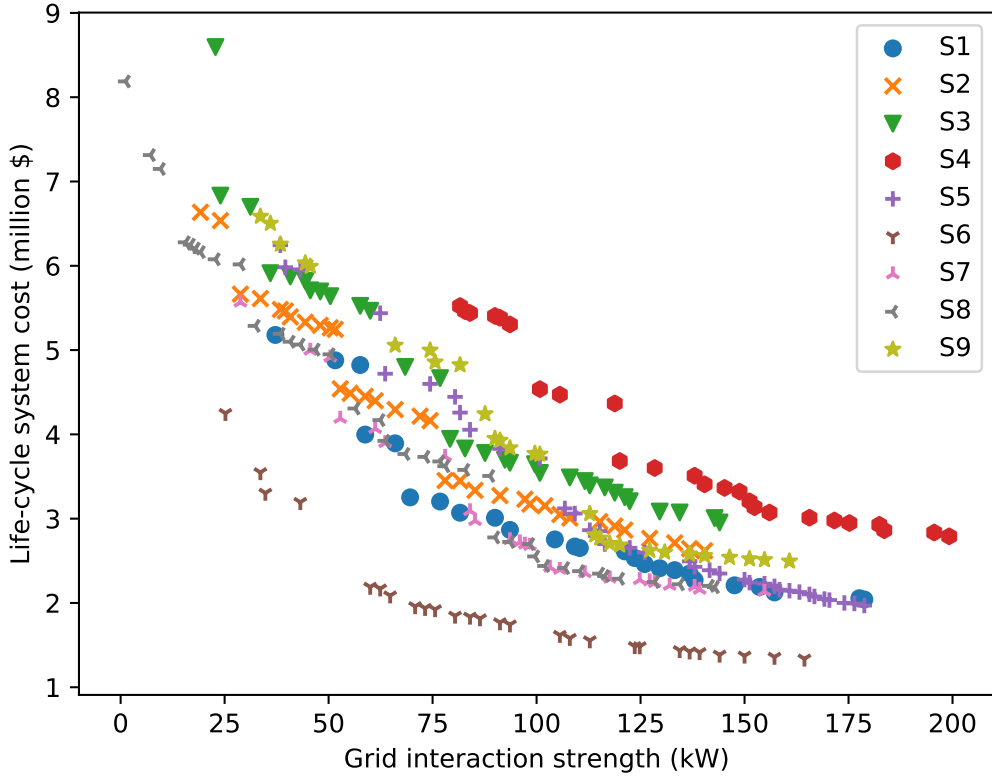


Figure 3: Pareto frontier of all DESs: system life-cycle cost versus grid interaction strength.

439 *4.2. Optimising the EI*

440 The present design of EI normally follows a sequential process, in which
 441 the design of each DES is first optimized (minimizing its LCC) individually
 442 considering a specified grid curtailment (upper bound for grid curtailments
 443 are given during the optimization process), and then, the grid is designed to
 444 accommodate the DESs. In this case, the configuration labeled as 25 will
 445 be chosen by each DES, because the grid curtailment is within a reasonable
 446 range. Then, the grid is designed to accommodate these energy systems. The

447 EI obtained by using this method is referred to as the reference EI (which
 448 is later used for comparison with the novel approach). For the reference EI,
 449 the grid is optimized by the model presented in Section 2.2.2.

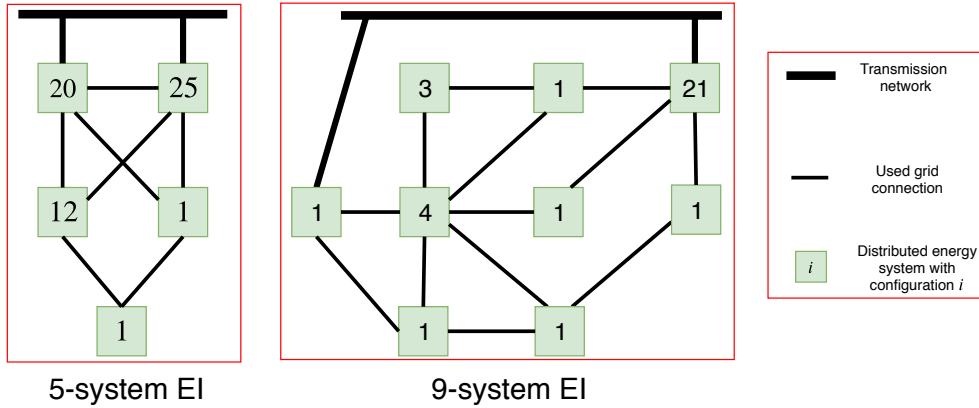


Figure 4: Optimal EI with five systems and nine systems. ‘1’ represents the most autonomous DES configuration while ‘25’ represents the least autonomous DES configuration

450 The optimal EIIs obtained by the novel approach are presented in Fig.
 451 4. For both cases, almost all DESs have an optimal configuration index
 452 different from the reference EI. DESs that are far away from the transmission
 453 line are more likely to choose an autonomous configuration (have an index
 454 close to 1) in order to reduce the cost of the grid. Consequently, for the
 455 EI obtained using the novel approach, there is a notable difference in the
 456 objective function values as well as the system configuration selected for
 457 most of the DESs when compared with the reference EI. It is interesting to
 458 analyze the impact on the overall cost due to the changes observed in the
 459 energy system design from the reference EI and the novel approach. The
 460 cost saving ratio (CSR) is proposed to quantify the cost difference between

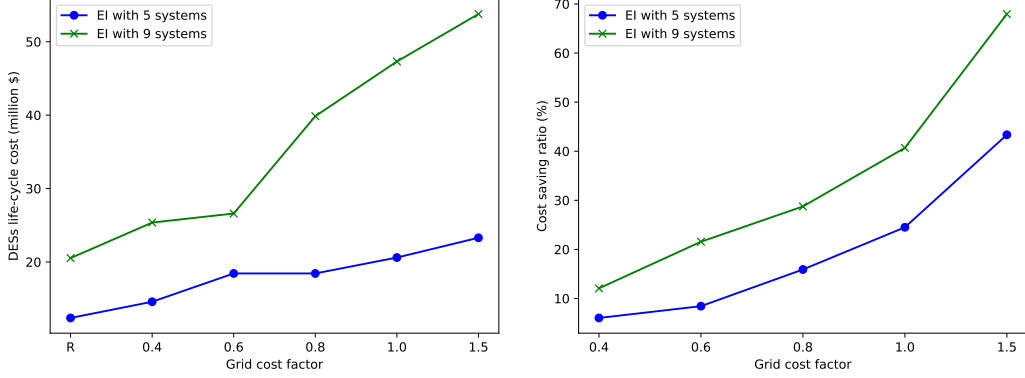
⁴⁶¹ the two models, as defined in Eq. (29)

$$CSR = (TC_r - TC_{opt}) / TC_{opt} \quad (29)$$

⁴⁶² In this equation, TC_r denotes the LCC of the reference EI while TC_{opt}
⁴⁶³ denotes the LCC of the optimal EI obtained from the novel method. The
⁴⁶⁴ LCC of the EI considers cash flows due to the grid as well as DESs. We
⁴⁶⁵ observe a CSR of 25% and 41% for EIs having 5 and 9 DESs, respectively,
⁴⁶⁶ which indicates that a significant cost reduction can be achieved by using
⁴⁶⁷ the novel approach introduced in this study. However, we need to under-
⁴⁶⁸ stand that these percentage improvements are highly sensitive to a number
⁴⁶⁹ of different factors.

⁴⁷⁰ 4.2.1. *Sensitivity of grid to DES cost ratio on the optimal EI*

⁴⁷¹ It is important to guarantee that the novel method introduced in this
⁴⁷² study performs well for a wider spectrum of scenarios. Therefore, it is es-
⁴⁷³ sential to analyze the factors that influence the optimal EI design and CSR,
⁴⁷⁴ such as the ratio of the grid cost to DES cost and the demand locations.
⁴⁷⁵ To begin the analysis, a constant grid cost factor is introduced to scale the
⁴⁷⁶ life-cycle cost of the grid. Grid cost factor is multiplied to the initial grid
⁴⁷⁷ cost, leading to a new grid cost. The objective of introducing a grid cost
⁴⁷⁸ factor is to study the performance of the novel optimization algorithm under
⁴⁷⁹ different grid to DES cost ratios. A grid cost factor higher than one indicates
⁴⁸⁰ that the investment and operation cost of the grid is higher than the initial
⁴⁸¹ case. Four scenarios are investigated (grid cost factor of 0.4, 0.6, 0.8, and
⁴⁸² 1.5). EI optimization is conducted independently under each grid cost factor
⁴⁸³ by using the novel method proposed in this study.



(a) LCC of DESs of the optimal EI under different grid cost factors (b) Cost saving ratio of the optimal EIs to reference EIs

Figure 5: The life-cycle cost of DESs of the optimal EIs under different grid cost factor and cost saving ratio of the optimal EIs. The ‘R’ in diagram (a) represents the reference case.

484 The LCC cost of DESs and CSR of our proposed method under different
 485 grid to DES cost ratios are first shown in Fig. 5. As indicated in Fig. 5a, the
 486 LCC of DESs of the optimal EIs increases with the increase in the grid cost
 487 factor (from 12 to 21 and 20 to 50 million USD for the EIs having five and nine
 488 DESs, respectively). A larger grid cost factor increases the marginal cost of
 489 the grid within the EI, which may lead to instances where the optimal DESs
 490 selected initially (grid cost factor = 1) become sub-optimal. To minimize
 491 the overall LCC, the optimal EI should depend less on the grid. According
 492 to Fig. 3, this requires DESs to be more autonomous, which requires more
 493 generation and storage infrastructures to be installed and maintained. As
 494 a result, the cost of DESs of the EI increases. In contrast, DESs will tend
 495 to depend more on the grid when the grid cost factor is low, because it is

496 cheaper to be connected to neighboring DESs and purchase energy generated
497 at a cheaper price. This will lead to less autonomous DESs, which will reduce
498 the LCC of the DESs. Hence, the change in the energy system and the grid
499 will depend on the marginal cost of the grid over DESs.

500 When looking at the cost saving effect of our proposed approach, we can
501 observe a reasonable CSR even when the grid cost factor is small, i.e., 0.4
502 (Fig. 5b). This indicates that the LCC of DESs obtained from the novel
503 method performs reasonably well compared to the reference EI. In addition,
504 the CSR becomes increasingly remarkable as the grid cost factor increases.
505 Most importantly, the CSR has a notably high value, indicating that the novel
506 method outperforms the reference EI by a significant margin. In general,
507 it is proven that the novel approach presented in this study performs well
508 compared to the reference method for a wider range of grid costs.

509 It is equally important to analyze the impact of the grid cost factor on
510 the entire EI, apart from being limited to the DESs. Optimal EIs obtained
511 for different grid cost factors are subsequently used to achieve this objective.
512 The LCC of these systems are computed for scenarios with grid cost factors
513 different from those that these systems are optimized for. Subsequently, the
514 LCC of these systems are compared with the optimal EI obtained considering
515 the specific grid cost factor. For example, the green line represents the LCC
516 of EIs when the grid cost factor is 0.4. The circle indicates the optimal EI
517 obtained for the specific cost factors. When moving from the red line to
518 the black one, the difference in LCCs for the optimal and the sub-optimal
519 scenarios notably increases. For example, the LCC increases from 47 to 62
520 million USD when the grid cost factor is 0.4 while it increases from 81 to 103

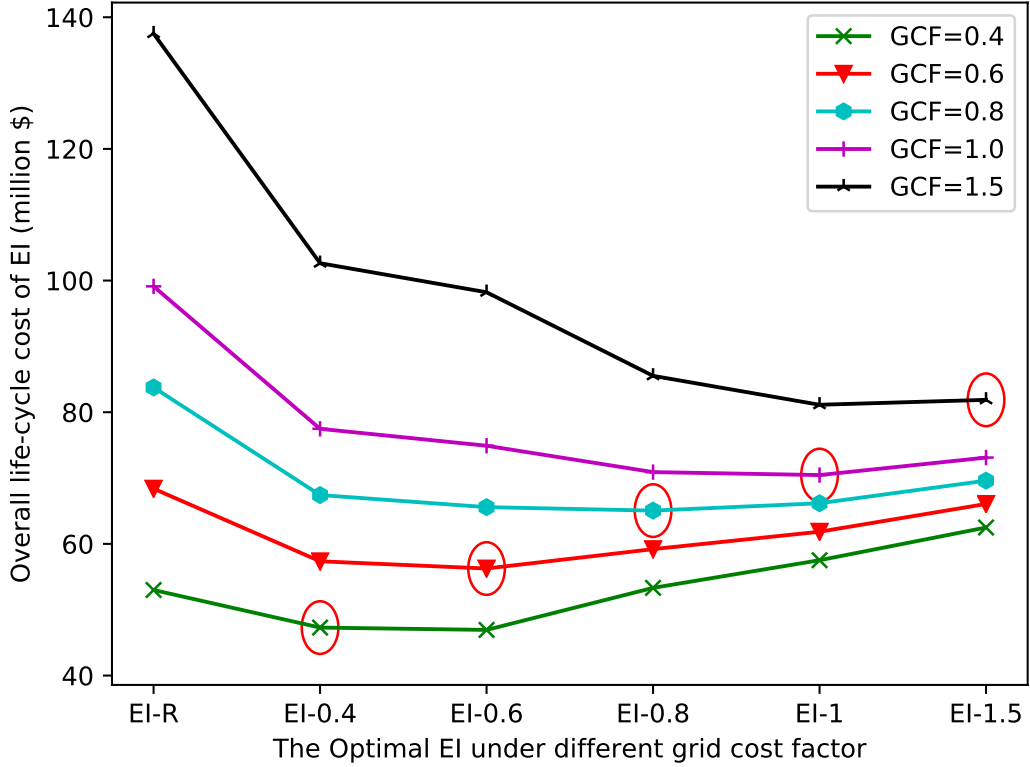


Figure 6: Life-cycle cost of different EIs under different grid cost factors (GCFs). The EIs are the optimal ones under specific GCFs indicated, while ‘EI-R’ represents the reference EI

521 million USD when the grid cost factor is 1.5. This clearly indicates that the
 522 design of the DESs has a notable impact on the LCC of the EI. This indicates
 523 that optimal selection of the DESs plays a vital role when minimizing the
 524 overall LCC of the EI. Mere selection of the lowest cost DES will result in
 525 a significant increase in the overall LCC. Therefore, the novel optimization
 526 algorithm will play a vital role for designing EIs in the future.

527 4.2.2. *Sensitivity of the DES location*

528 Locations of the DESs can have a notable impact on the grid and the EI.
529 It is therefore important to guarantee that the novel optimization method
530 can yield the optimal solutions for any arrangement made within the EI,
531 irrespective of the location. In order to analyze this, locations of the DESs
532 introduced in Fig. 2 swapped and the integrated EI optimization is conducted
533 accordingly. The optimal grid LCC (denoted as GC), DESs LCC (SC), and
534 overall LCC of the optimal EI s ($TC - Opt$) and reference EI s ($TC - R$) are
535 shown in Fig. 7.

536 The figure suggests that the grid cost (GC) changes notably with respect
537 to the demand locations. This clearly indicates that changes in the DES
538 locations can be costly in terms of the grid. However, the LCC of DESs
539 moves in an opposite direction to that of Grid LCC, which implies that the
540 design of DESs can be altered accordingly in order to reduce the direct impact
541 due to the location changes. The significant difference observed between the
542 TC-R and TC-Opt suggests that the novel method introduced in this study
543 can help to adapt both grid and DESs accordingly, which will notably reduce
544 the LCC of the EI. As a result, the CSR varies from (Fig. 8) 20% to 60%
545 when comparing the LCC obtained from the novel method with that from
546 the reference EI. Therefore, it can be concluded that the novel method can
547 optimize the EI irrespective of the location of the DESs with a significant
548 margin when considering the LCC of the EI.

549 4.3. *N-1 security*

550 In this section, the cost and benefit of n-1 security of the grid are stud-
551 ied. The grid must construct extra lines to ensure n-1 security. Rather than

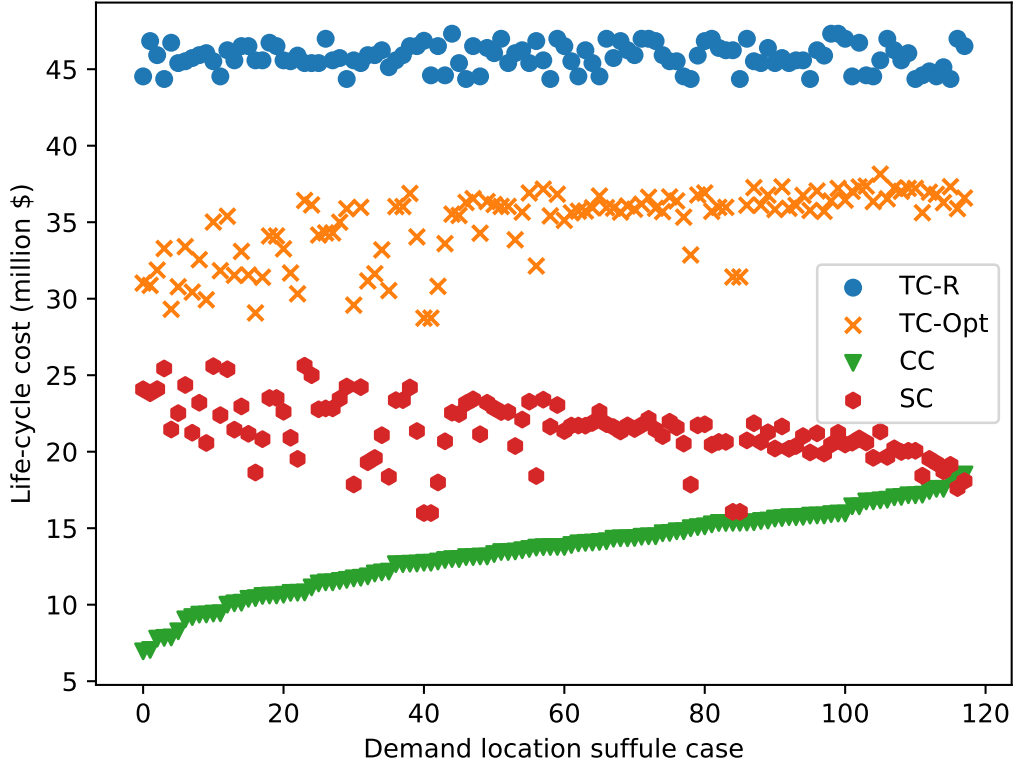


Figure 7: Impact of demand locations on the optimal system, grid, and overall life-cycle cost of the optimal EI. ‘TC-R’ represents the overall LCC of reference EIs, ‘TC-Opt’ represents the LCC of the EIs optimized by the novel approach, ‘GC’ represents the grid LCC, and the ‘SC’ represents the LCC of DESs

552 comparing the differences between the grids directly, we compute the cost in-
 553 crement introduced by n-1 security. To determine the benefits of n-1 security,
 554 the loss of load probability (LoLP) is computed under assumed contingencies
 555 to demonstrate the operational reliability of the EI with n-1 security. The
 556 results show that although the grid cost will increase remarkably, the gained
 557 operational reliability justifies the extra cost.

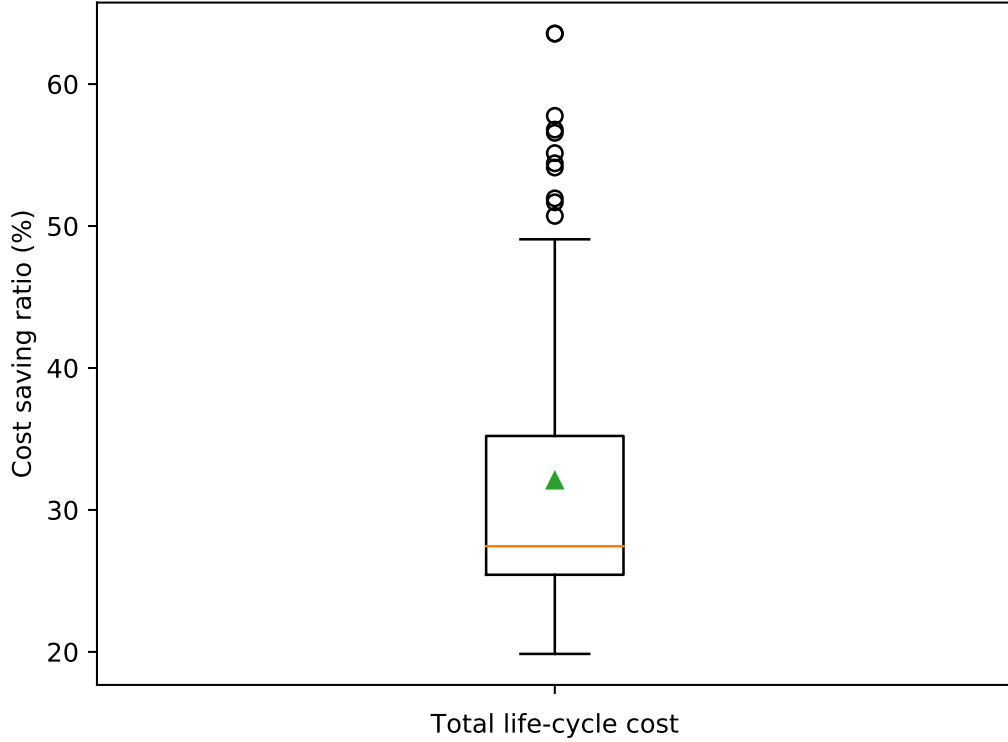


Figure 8: Cost saving ratio distribution of integrated EI optimization under different demand locations. One point of the plot is obtained by one specific demand location

558 4.3.1. *n-1 security of the EI*

559 Consideration of the n-1 security at the design phase is a novel feature
 560 introduced in the optimization algorithm presented in this study. On one
 561 hand, to ensure the n-1 security, additional power lines need to be constructed
 562 among DESs, which add additional cost component to the EI. Hence, this
 563 section is first dedicated to understanding the cost of ensuring the n-1 security
 564 of the EI. On the other hand, ensuring n-1 security increases the reliability
 565 of the EI to unfavorable contingency. Thus, the second half of this section

566 is devoted towards investigating the importance of introducing n-1 security
567 from the power supply reliability perspective, where EIs with n-1 security
568 are compared to EIs without n-1 security.

569 Optimizing the grid considering n-1 security is a challenging task. n-1
570 security adds an additional cost component into the LCC of the EI. There-
571 fore, it is important to evaluate the cost increment due to the introduction
572 of n-1 security. The percentage increase in the grid LCC is computed for
573 1000 randomly sampled DES configuration combinations where the grid is
574 optimized with and without n-1 security. Figure 9 shows that the grid LCC
575 increment ranges from 90% to 130% and 130% to 180% for EIs with five and
576 nine DESs, respectively.

577 The cost analysis clearly shows that n-1 security adds a significant cost
578 component to the EI. Therefore, it is important to evaluate the necessity of
579 n-1 security. When n-1 security is not enforced, the optimal grid connection
580 usually ends up being radial (Fig. 10). As a result, a part of the EI must
581 operate in an island mode whenever a contingency takes place. This can lead
582 to a significant increase in the LOLP, which quantifies the energy demand
583 failed during a contingency. The EI might be capable to cater to the demand
584 in a robust manner whenever the n-1 security is guaranteed. Hence, LoLP
585 can be regarded as the benefit of ensuring n-1 security. In this study, LOLP
586 is defined according to Eq. (30),

$$\left(\sum_t lol^t \right) / \left(\sum_t d^t \right) \quad (30)$$

587 Where lol^t is the lost of load and d^t is the demand of the isolated DES at
588 time t .

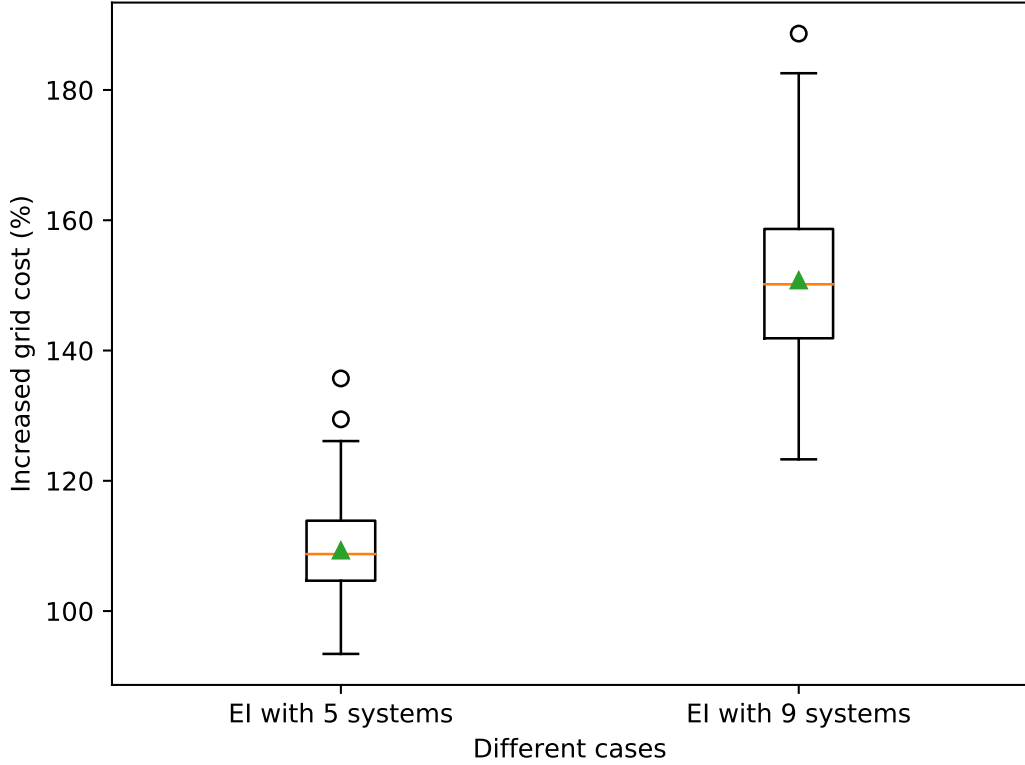


Figure 9: Cost of n-1 security for different sizes of EIs under different demand profiles

589 During a contingency where several DESs of an EI are disconnected from
 590 the transmission system but are connected with each other, the disconnected
 591 DESs can cooperate with each other to cater as much the demand as possible.
 592 However, it might be inevitable that there is load that needs to be curtailed.
 593 Quantifying the LOLP in this case is a difficult problem. Therefore, to sim-
 594 plify the assessment, we introduced nodes which entirely represent demand.
 595 Under grid contingency, demand nodes are catered by the DES to which
 596 they are connected. Through analyzing the catered demand in the demand
 597 node, we could estimate the energy supplement potential among DESs. To-

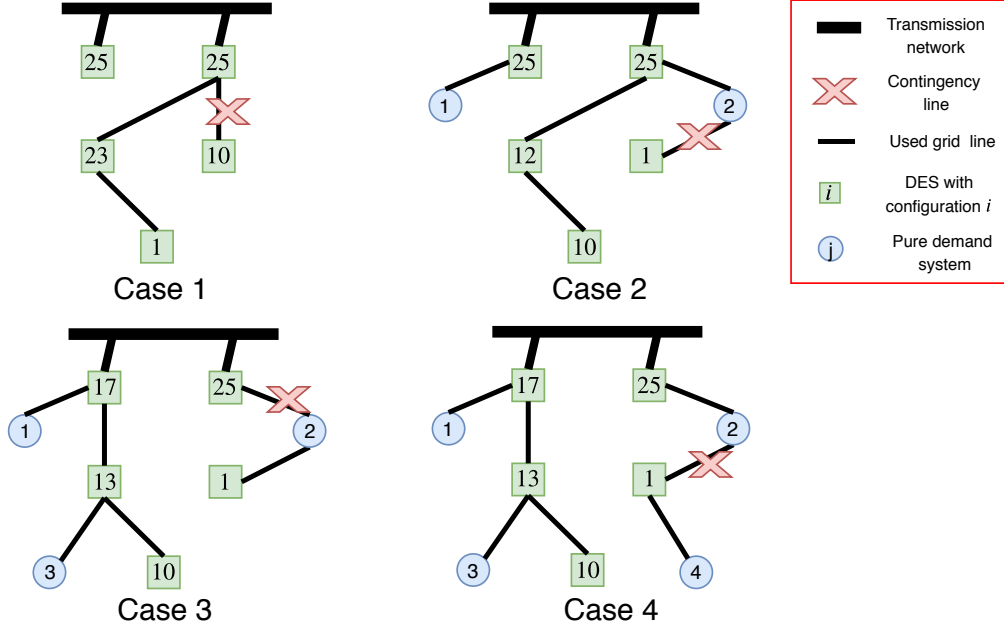


Figure 10: Optimal EI without n-1 security and assumed contingency cases for the reliability study

wards this end, four contingency cases of the five-system EI, which is not n-1 secured (Fig. 10) are adopted for demonstration.

Table 1 presents the LOLP of the demand nodes during the break down in the grid. When comparing Cases 1 and 2, with the same demands but different autonomy levels, we see that an EI without n-1 security can have a large LoLP. When there are pure demand nodes connected, the reliability of the EI can be compromised considerably, as shown by the significant LoLP increment of over 40% in Cases 3 and 4. This indicates that there is a very high probability of a drop in power supply reliability during a breakdown in the connection line. This makes it essential to move beyond simply optimizing the EI and consider n-1 security. The optimization algorithm presented

Table 1: Loss of load probability of the EI without N-1 security under assumed contingency cases

Case	Total demand (GWh)	Loss of load (GWh)	Loss of load (%)	Total pure demand (GWh)	Severed pure demand (GWh)	Served ratio (%)
1	1.20	0.33	27.61			
2	1.20	0.11	9.31			
3	2.13	0.86	40.40	0.93	0.18	19.35
4	2.41	1.09	45.30	1.21	0.23	19.01

609 in this study presents a novel method to consider n-1 security during the EI
 610 optimization.

611 5. Conclusion

612 This study introduces a novel optimization algorithm to design robust
 613 EIs. A two-step integrated optimization model is used, in which the first
 614 step presents a Pareto optimal set of configurations for each DES. The sec-
 615 ond step formulates a bi-level optimization algorithm to select the optimal
 616 configuration of DESs (out of the set of Pareto solutions) and the connection
 617 of the grid, while guaranteeing n-1 security.

618 When compared to other methods used in the present state-of-the-art,
 619 this novel optimization method can reduce the overall life-cycle cost by 20%
 620 to 60% depending on the demand location. The results show that the LCC of
 621 each EI can be notably influenced by the autonomy level of the adopted DESs.
 622 Therefore, it is important to consider the autonomy level of the energy system

623 along with its connectivity to the EI design simultaneously. The sensitivity
624 of energy system location and the grid cost is subsequently analyzed. It
625 was shown that both the aforementioned factors notably influence the overall
626 LCC of the EI. The LCC can notably increase in certain instances while using
627 the present EI design approach. However, the novel approach presented in
628 this study can mitigate the increase in the life-cycle cost, which ends up
629 leading to a cost saving ratio of up to 60%. In addition, simulations show
630 that ensuring n-1 security of the EI is necessary to reinforce the EI reliability.
631 Moreover, the optimal DES configurations of the EI suggest that DESs can be
632 introduced as a substitution to the grid expansion when the energy demand
633 increases.

634 In the future, this work can be extended to consider cooperative operation
635 among DESs within the EI. In addition, evaluation of the EI reliability under
636 unfavorable contingencies is critical for further EI design solutions. Further
637 investigation on the trade-off between the autonomy and the security of the
638 EI could be interesting for future energy systems.

639 References

- 640 G. E. Alvarez, M. G. Marcovecchio, and P. A. Aguirre. Security constrained
641 unit commitment scheduling: A new MILP formulation for solving trans-
642 mission constraints. *Computers and Chemical Engineering*, 115:455–473,
643 2018. ISSN 00981354. doi: 10.1016/j.compchemeng.2018.05.001. URL
644 <https://doi.org/10.1016/j.compchemeng.2018.05.001>.
- 645 J. Álvarez López, J. L. Ceciliano-Meza, I. Guillén, and R. Nieva Gómez.
646 A Heuristic algorithm to solve the unit commitment problem for real-life

- 647 large-scale power systems. *International Journal of Electrical Power and*
648 *Energy Systems*, 49(1):287–295, 2013. ISSN 01420615. doi: 10.1016/j.
649 ijepes.2013.01.016.
- 650 T. Bengtsson, P. Bickel, and B. Li. Curse-of-dimensionality revisited : Col-
651 lapse of the particle filter in very large scale systems. *Probability and*
652 *Statistics: Essays in Honor of David A. Freedman*, 2:316–334, 2008. doi:
653 10.1214/193940307000000518.
- 654 S. Binato, M. V. F. Pereira, and S. Granville. A new Benders decomposition
655 approach to solve power transmission network design problems. *Power*
656 *Systems, IEEE Transactions on*, 16(2):235–240, may 2001. ISSN 0885-
657 8950.
- 658 H. Gharavi, M. M. Ardehali, and S. Ghanbari-Tichi. Imperial competitive
659 algorithm optimization of fuzzy multi-objective design of a hybrid green
660 power system with considerations for economics, reliability, and environ-
661 mental emissions. *Renewable Energy*, 78:427–437, 2015. ISSN 18790682.
662 doi: 10.1016/j.renene.2015.01.029. URL <http://dx.doi.org/10.1016/j.renene.2015.01.029>.
- 664 L. Gong, C. Wang, C. Zhang, and Y. Fu. High-Performance Computing based
665 Fully Parallel Security-Constrained Unit Commitment with Dispatchable
666 Transmission Network. *IEEE Transactions on Power Systems*, 34(2):931–
667 941, 2018. ISSN 08858950. doi: 10.1109/TPWRS.2018.2876025.
- 668 R. A. Jabr. Robust transmission network expansion planning with uncertain

- 669 renewable generation and loads. *IEEE Transactions on Power Systems*, 28
670 (4):4558–4567, 2013. ISSN 08858950. doi: 10.1109/TPWRS.2013.2267058.
- 671 B. Jeddi, V. Vahidinasab, P. Ramezanpour, and J. Aghaei. Electrical Power
672 and Energy Systems Robust optimization framework for dynamic dis-
673 tributed energy resources planning in distribution networks. *Electr. Power*
674 *Energy Syst.*, 110(March):419–433, 2019. ISSN 0142-0615. doi: 10.1016/j.
675 ijepes.2019.03.026. URL <https://doi.org/10.1016/j.ijepes.2019.03.026>.
- 676 R. Jing, M. Wang, Z. Zhang, X. Wang, N. Li, N. Shah, and Y. Zhao.
677 Distributed or centralized? Designing district-level urban energy sys-
678 tems by a hierarchical approach considering demand uncertainties. *Ap-*
679 *plied Energy*, 252(June):113424, 2019. ISSN 03062619. doi: 10.1016/j.
680 apenergy.2019.113424. URL [https://linkinghub.elsevier.com/retrieve/pii/
681 S0306261919310980](https://linkinghub.elsevier.com/retrieve/pii/S0306261919310980).
- 682 A. Kaveh. *Advances in metaheuristic algorithms for optimal design of*
683 *structures, second edition*. Springer, 2016. ISBN 9783319461731. doi:
684 10.1007/978-3-319-46173-1.
- 685 M. Le Guen, L. Mosca, A. T. D. Perera, S. Cocco, and N. Mohajeri. Im-
686 proving the energy sustainability of a Swiss village through building ren-
687 ovation and renewable energy integration. *Energy & Buildings*, 158:906–
688 923, 2018. ISSN 0378-7788. doi: 10.1016/j.enbuild.2017.10.057. URL
689 <http://dx.doi.org/10.1016/j.enbuild.2017.10.057>.
- 690 L. Li, H. Mu, N. Li, and M. Li. Economic and environmental optimization for
691 distributed energy resource systems coupled with district energy networks.

- 692 *Energy*, 109:947–960, 2016. ISSN 0360-5442. doi: 10.1016/j.energy.2016.
693 05.026. URL <http://dx.doi.org/10.1016/j.energy.2016.05.026>.
- 694 M. Li, L. Liu, and D. Lin. A fast steady-state ϵ -dominance multi-objective
695 evolutionary algorithm. *Comput. Optim. Appl.*, 48(1):109–138, 2011. ISSN
696 09266003. doi: 10.1007/s10589-009-9241-x.
- 697 J. Á. López, J. L. Cecilio-Meza, I. Guillén Moya, and R. Nieva Gómez.
698 A MIQCP formulation to solve the unit commitment problem for large-
699 scale power systems. *International Journal of Electrical Power and Energy
700 Systems*, 36(1):68–75, 2012. ISSN 01420615. doi: 10.1016/j.ijepes.2011.10.
701 025.
- 702 A. Lorestani and M. M. Ardehali. Optimization of autonomous combined
703 heat and power system including PVT , WT , storages , and electric heat
704 utilizing novel evolutionary particle swarm optimization algorithm. *Renewable
705 Energy*, 119:490–503, 2018a. ISSN 0960-1481. doi: 10.1016/j.
706 renene.2017.12.037. URL <https://doi.org/10.1016/j.renene.2017.12.037>.
- 707 A. Lorestani and M. M. Ardehali. Optimal integration of renewable en-
708 ergy sources for autonomous tri-generation combined cooling , heating
709 and power system based on evolutionary particle swarm optimization al-
710 gorithm. *Energy*, 145:839–855, 2018b. ISSN 0360-5442. doi: 10.1016/j.
711 energy.2017.12.155. URL <https://doi.org/10.1016/j.energy.2017.12.155>.
- 712 S. Lumbrieras, A. Ramos, and F. Banez-Chicharro. Optimal transmission
713 network expansion planning in real-sized power systems with high re-
714 newable penetration. *Electric Power Systems Research*, 149:76–88, aug

- 715 2017. ISSN 03787796. doi: 10.1016/j.epsr.2017.04.020. URL <http://dx.doi.org/10.1016/j.epsr.2017.04.020><https://linkinghub.elsevier.com/retrieve/pii/S0378779617301670>.
- 718 D. E. Majewski, M. Wirtz, M. Lampe, and A. Bardow. Robust multi-
719 objective optimization for sustainable design of distributed energy sup-
720 ply systems. *Computers and Chemical Engineering*, 102:26–39, 2017.
721 ISSN 0098-1354. doi: 10.1016/j.compchemeng.2016.11.038. URL <http://dx.doi.org/10.1016/j.compchemeng.2016.11.038>.
- 723 F. Martel, Y. Dubé, S. Kelouwani, J. Jaguemont, and K. Agbossou. Long-
724 term assessment of economic plug-in hybrid electric vehicle battery life-
725 time degradation management through near optimal fuel cell load shar-
726 ing. *Journal of Power Sources*, 318:270–282, 2016. ISSN 03787753. doi:
727 10.1016/j.jpowsour.2016.04.029.
- 728 R. Mínguez and R. García-bertrand. Robust transmission network ex-
729 pansion planning in energy systems : Improving computational perfor-
730 mance. *European Journal of Operational Research*, 248:21–32, 2016. doi:
731 10.1016/j.ejor.2015.06.068.
- 732 S. Mishra, C. Bordin, A. Tomasdard, and I. Palu. A multi-agent system ap-
733 proach for optimal microgrid expansion planning under uncertainty. *Int. J.*
734 *Electr. Power Energy Syst.*, 109(January):696–709, 2019. ISSN 01420615.
735 doi: 10.1016/j.ijepes.2019.01.044. URL <https://doi.org/10.1016/j.ijepes.2019.01.044>.
- 737 A. Moreira, D. Pozo, A. Street, and E. Sauma. Reliable Renewable Genera-

- 738 tion and Transmission Expansion Planning: Co-Optimizing System's Re-
739 sources for Meeting Renewable Targets. *IEEE Transactions on Power Sys-*
740 *tems*, 32(4):3246–3257, jul 2017. ISSN 0885-8950. doi: 10.1109/TPWRS.
741 2016.2631450. URL <http://ieeexplore.ieee.org/document/7752917/>.
- 742 B. Morvaj, R. Evins, and J. Carmeliet. Optimization framework for dis-
743 tributed energy systems with integrated electrical grid constraints. *Applied*
744 *Energy*, 171:296–313, 2016. ISSN 0306-2619. doi: 10.1016/j.apenergy.2016.
745 03.090. URL <http://dx.doi.org/10.1016/j.apenergy.2016.03.090>.
- 746 G. A. Orfanos, P. S. Georgilakis, and N. D. Hatziargyriou. Transmission
747 Expansion Planning of Systems With Increasing Wind Power Integration.
748 *IEEE Transactions on Power Systems*, 28(2):1355–1362, may 2013. ISSN
749 0885-8950. doi: 10.1109/TPWRS.2012.2214242. URL <http://ieeexplore.>
750 [ieee.org/document/6313960/](http://ieeexplore.ieee.org/document/6313960/).
- 751 P. Paliwal, N. P. Patidar, and R. K. Nema. Determination of reliability
752 constrained optimal resource mix for an autonomous hybrid power system
753 using Particle Swarm Optimization. *Renewable Energy*, 63:194–204, 2014.
754 ISSN 09601481. doi: 10.1016/j.renene.2013.09.003. URL <http://dx.doi.>
755 [org/10.1016/j.renene.2013.09.003](http://dx.doi.org/10.1016/j.renene.2013.09.003).
- 756 A. Perera, V. M. Nik, P. Wickramasinghe, and J.-L. Scartezzini. Re-
757 defining energy system flexibility for distributed energy system design.
758 *Appl. Energy*, 253:113572, nov 2019. ISSN 03062619. doi: 10.1016/j.
759 apenergy.2019.113572. URL <https://linkinghub.elsevier.com/retrieve/pii/>
760 S0306261919312462.

- 761 A. T. Perera, S. Cocco, J. L. Scartezzini, and D. Mauree. Quantifying
762 the impact of urban climate by extending the boundaries of urban energy
763 system modeling. *Applied Energy*, 222(December 2017):847–860, 2018.
764 ISSN 03062619. doi: 10.1016/j.apenergy.2018.04.004. URL <https://doi.org/10.1016/j.apenergy.2018.04.004>.
- 766 A. T. D. Perera, V. M. Nik, D. Mauree, and J.-L. Scartezzini. Electrical hubs:
767 An effective way to integrate non-dispatchable renewable energy sources
768 with minimum impact to the grid. *Applied Energy*, 190(Supplement C):
769 232–248, 2017a. ISSN 0306-2619. doi: <https://doi.org/10.1016/j.apenergy.2016.12.127>. URL <http://www.sciencedirect.com/science/article/pii/S0306261916319109>.
- 772 A. T. D. Perera, V. M. Nik, D. Mauree, and J.-l. Scartezzini. An integrated
773 approach to design site specific distributed electrical hubs combining
774 optimization , multi-criterion assessment and decision making. *Energy*,
775 134:103–120, 2017b. ISSN 0360-5442. doi: 10.1016/j.energy.2017.06.002.
776 URL <http://dx.doi.org/10.1016/j.energy.2017.06.002>.
- 777 A. Poullikkas. Sustainable options for electric vehicle technologies. *Renewable
778 and Sustainable Energy Reviews*, 41:1277–1287, 2015. ISSN 13640321. doi:
779 10.1016/j.rser.2014.09.016. URL [http://dx.doi.org/10.1016/j.rser.2014.09.
780 016](http://dx.doi.org/10.1016/j.rser.2014.09.016).
- 781 H. Ren, Y. Lu, Q. Wu, X. Yang, and A. Zhou. Multi-objective
782 optimization of a hybrid distributed energy system using NSGA-II
783 algorithm. *Frontiers in Energy*, 12(4):518–528, dec 2018. ISSN
784 2095-1701. doi: 10.1007/s11708-018-0594-7. URL <http://doi.org/10.1007/s11708-018-0594-7>.

- 785 1007/s11708-018-0594-7{%}0ARESEARCHARTICLEHongbohttp://link.springer.com/10.1007/s11708-018-0594-7.
- 787 C. Roldán, A. Sánchez de la Nieta, R. García-Bertrand, and R. Mínguez. Robust dynamic transmission and renewable generation expansion planning: Walking towards sustainable systems. *International Journal of Electrical Power & Energy Systems*, 96(September 2017):52–63, mar 2018. ISSN 01420615. doi: 10.1016/j.ijepes.2017.09.021. URL <https://doi.org/10.1016/j.ijepes.2017.09.021><https://linkinghub.elsevier.com/retrieve/pii/S0142061517303083>.
- 794 R. Romero, A. Monticelli, A. Garcia, and S. Haffner. Test systems and mathematical models for transmission network expansion planning. *IEE Proceedings: Generation, Transmission and Distribution*, 149(1):27–36, jan 2002. ISSN 13502360.
- 798 S. Twaha and M. A. M. Ramli. A review of optimization approaches for hybrid distributed energy generation systems : Off-grid and grid-connected systems. *Sustainable Cities and Society*, 41(April):320–331, 2018. ISSN 2210-6707. doi: 10.1016/j.scs.2018.05.027. URL <https://doi.org/10.1016/j.scs.2018.05.027>.
- 803 F. Varasteh, M. S. Nazar, A. Heidari, M. Shafie-khah, and J. P. Catalão. Distributed energy resource and network expansion planning of a CCHP based active microgrid considering demand response programs. *Energy*, 172:79–105, apr 2019. ISSN 03605442. doi: 10.1016/j.energy.2019.01.015. URL <https://linkinghub.elsevier.com/retrieve/pii/S0360544219300179>.

- 808 P. Vilaça Gomes, J. T. Saraiva, L. Carvalho, B. Dias, and L. W. Oliveira.
809 Impact of decision-making models in Transmission Expansion Planning
810 considering large shares of renewable energy sources. *Electr. Power Syst.*
811 *Res.*, 174(April):105852, 2019. ISSN 03787796. doi: 10.1016/j.epsr.2019.
812 04.030. URL <https://doi.org/10.1016/j.epsr.2019.04.030>.
- 813 X. Wang and K.-t. Fang. The effective dimension and quasi-Monte Carlo.
814 *Journal of Complexity*, 19:101–124, 2003. doi: 10.1016/S0885-064X(03)
815 00003-7.
- 816 P. Wu, H. Cheng, and J. Xing. The Interval Minimum Load Cutting Problem
817 in the Process of Transmission Network Expansion Planning Considering
818 Uncertainty in Demand. *Power Systems, IEEE Transactions on*, 23(3):
819 1497–1506, aug 2008. ISSN 0885-8950.
- 820 N. Yang and F. Wen. A chance constrained programming approach to trans-
821 mission system expansion planning. *Electric Power Systems Research*,
822 75(2):171–177, 2005. ISSN 0378-7796. doi: <https://doi.org/10.1016/j.epsr.2005.02.002>. URL <http://www.sciencedirect.com/science/article/pii/S037877960500101X>.
- 825 H. Yu, C. Chung, K. Wong, and J. Zhang. A Chance Constrained Trans-
826 mission Network Expansion Planning Method With Consideration of Load
827 and Wind Farm Uncertainties. *IEEE Transactions on Power Systems*, 24
828 (3):1568–1576, aug 2009. ISSN 0885-8950. doi: 10.1109/TPWRS.2009.
829 2021202. URL <http://ieeexplore.ieee.org/document/4909013/>.
- 830 S. Zymler, D. Kuhn, and B. Rustem. Distributionally robust joint chance

831 constraints with second-order moment information. *Mathematical Opti-*
832 *mization Society*, pages 167–198, 2013. doi: 10.1007/s10107-011-0494-7.